13

Rock-Fluid Interaction Along Seismogenic Faults Infered from Clay Minerals in Okitsu Mélange, the Cretaceous Shimanto Belt, SW Japan

Yoshitaka Hashimoto and Umihiko Kaji
Kochi Univeristy
Japan

1. Introduction

Rock-fluid interactions along seismogenic faults are significant issues, because they are strongly related to seismogenic mechanisms and also to modifications of the seismogenic fault itself. Various mechanisms for seismogenesis have been proposed, such as frictional melting (Sibson, 1975; Spray, 1992), thermal pressurization (Mase and Smith, 1987; Melosh, 1979; O'Hara et al., 2006; Sibson, 1977; Wibberley and Shimamoto, 2005), acoustic fluidization (Melosh, 1979; Otsuki et al., 2003), elastohydrodynamic lubrication (Brodsky and Kanamori, 2001), and silica gel lubrication (Di Toro et al., 2006). Some of these are related to frictional heating. Heating signatures from natural faults have been well-studied on the basis of the remaining grains in pseudotachylyte along faults (Ikesawa et al., 2003; Ujiie et al., 2007), the vitrinite reflectance anomaly (O'Hara et al., 2006), borehole logging (Kano et al., 2006; Mishima et al., 2006; Tanaka et al., 2006), the thermal decomposition of paramagnetic minerals (Mishima et al., 2006), and the distribution of minor elements (Ishikawa et al., 2008). In addition to the thermal effects, some of the seismogenic mechanisms are also strongly related to rock-fluid interactions. Studies focusing on rock-fluid interactions along fossil seismogenic faults have been conducted at some major fault zones. These include the Nojima fault in Japan (an intra-crustal seismogenic fault), where bulk rock chemistry analysis was used (Tanaka et al., 2007), the Chi-Chi fault in Taiwan (an active subduction plate boundary fault), which was studied on the basis of its clay characteristics (Hashimoto et al., 2008; Hashimoto et al., 2007), fossil faults such as the Mugi mélange, in the Shimanto Belt, Japan, again using bulk rock chemistry (Hashimoto et al., 2009), and an out of sequence thrust in the Shimanto Belt, Japan, using minor element distributions (Honda et al., 2011; Yamaguchi et al., 2011).

In this study, we focused on clay minerals within the fossil seismogenic fault along the subduction interface, in order to understand rock-fluid interactions at the fault. Clay minerals are commonly produced along faults, possibly by alteration of fine-grained abraded host rock materials due to rock-fluid interaction. The characteristics of clay minerals along seismogenic faults, in comparison with those of host rocks, provide clues

to help understand rock-fluid interactions at the time of seismogenesis or related phenomena.
The studied fault is a fossil seismogenic fault along a subduction interface, in the Okitsu melange, the Cretaceous Shimanto Belt, SW Japan. The Shimanto Belt is the most studied on-land accretionary complex in the world, with lithology, age, thermal structure, and deformation structures available. These studies have revealed that the Shimanto Belt includes a deformation along its subduction interface from underthrusting to underplating, and that the Shimanto Belt is experienced at the seismogenic depth on the basis of the thermal model for seismogenic zones (Hyndman and Wang, 1993; Oleskevich et al., 1999). At the northernmost boundary fault of the Okitsu melange, the first pseudotachylyte within the sedimentary rocks was reported (Ikesawa et al., 2003), indicating that the fault was formed by melt lubrication along the subduction interface.
We conducted an X-ray diffraction (XRD) analysis on the host and fault rocks along the fossil seismogenic fault, and examined mineralogy, iron and magnesium substitution in chlorite, illite crystallinity, and semi-quantification of illite and chlorite to determine the clay characteristics for seismogenic fault rocks, in comparison with those of the host rocks. Finally, characteristic rock-fluid interactions in seismogenic faults, due to melt lubrication along the subduction interface, are discussed.

2. Geological setting of Okitsu melange and the northern boundary fault zone with pseudotachylytes

The Shimanto Belt is an ancient accretionary complex exposed on land from the Kanto region to the Okinawa islands, Japan, almost parallel to the Nankai Trough (Fig. 1). The Shimanto Belt is divided into two units on the basis of age, the northern Cretaceous Unit and the southern Tertiary Unit (Taira et al., 1988) (Fig. 1A). On Shikoku Island, the 4th largest island in Japan, the Shimanto Belt is bounded by the Butsuzo Tectonic Line from the Chichibu Belt, a Jurassic accretionary complex (Fig. 1B), and is further classified by its lithology as a melange unit and a coherent unit (Taira et al., 1988) (Fig. 1B). A melange unit is composed of chaotic rocks representing blocks in matrix textures. Most of the melange in the Shimanto Belt is tectonic in origin (e.g., Kimura and Mukai, 1991; Onishi and Kimura, 1995; Hashimoto and Kimura, 1999). A coherent unit is composed mainly of an alternation of sandstone and mudstone with weaker deformations (Taira et al.1988).
The study area is in the Okitsu mélange, Shikoku Island, SW Japan. The Okitsu melange is located at the southern end of the Cretaceous Unit (Fig. 1). The main lithology of the Okitsu melange is sandstone and black shale showing tectonic melange textures, minor basalts, cherts, red shale, and tuff. Foliations are well developed within the shale matrices. The mélange foliations strike ENE–WSW and dip steeply to the north. The radiolarian age of the Okitsu melange is Cenomanian to Turonian from cherts, and Santonian to Campanian from black shale (Taira et al., 1988). The paleo-maximum temperature of the mélange is about 270 (± 30)°C, based on vitrinite reflectance (Sakaguchi, 1999).
The northern boundary fault bounds the Okitsu mélange from Nonokawa formation, a coherent unit in the north (Fig. 1B). The fault zone is about 5–10 m wide (Fig. 2), and mainly develops within the Okitsu melange. Basalt blocks, and black shale matrices mixed with tuffaceous shale in some parts, are included within the fault zone, which strikes ENE–WSW, almost parallel to the melange foliations (Fig. 2).

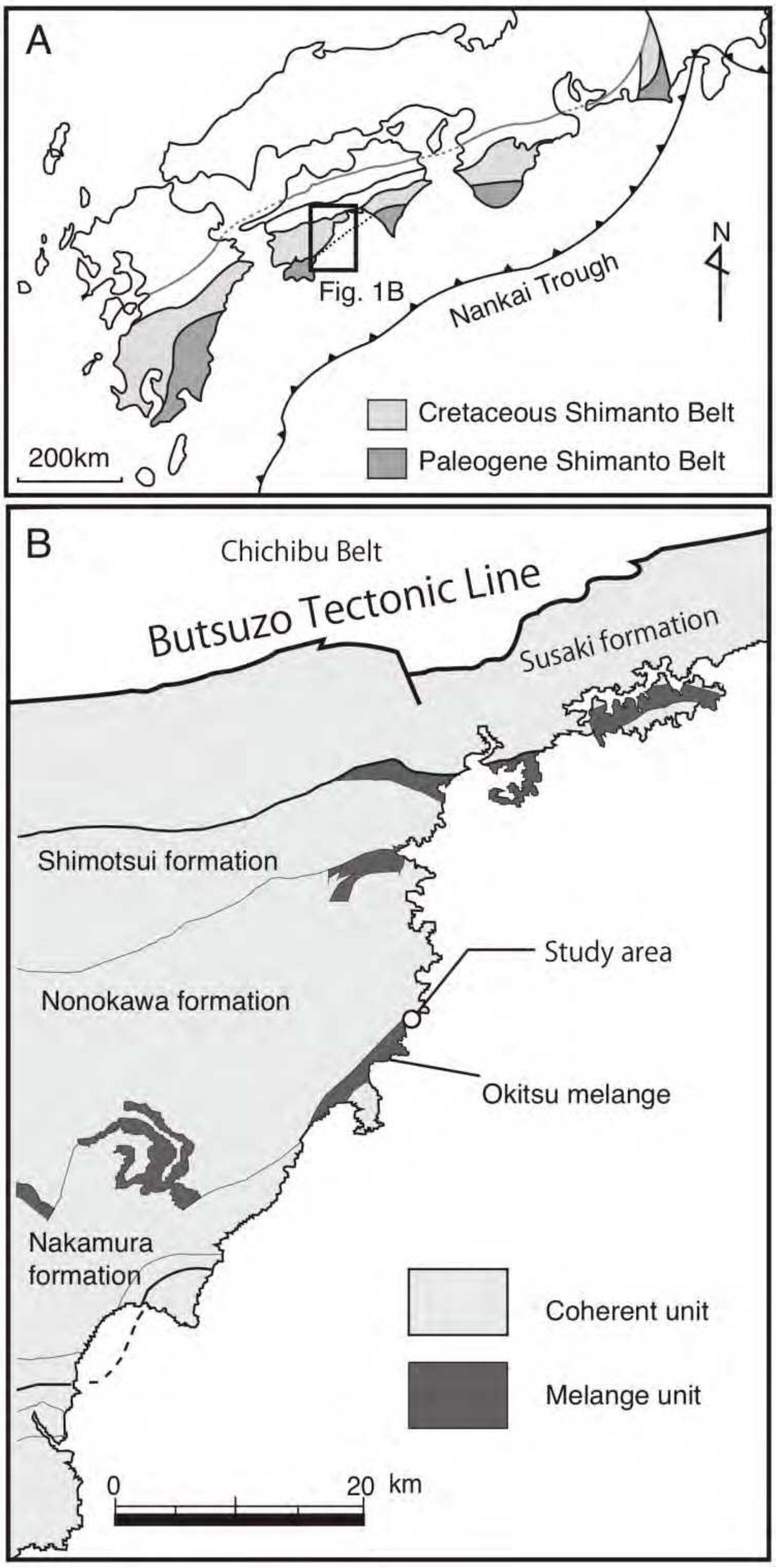

Fig. 1. A) Distribution of the Shimanto Belt along SW Japan. B) Distribution of mélange and coherent units in SW Shikoku Island. Study area is also shown.

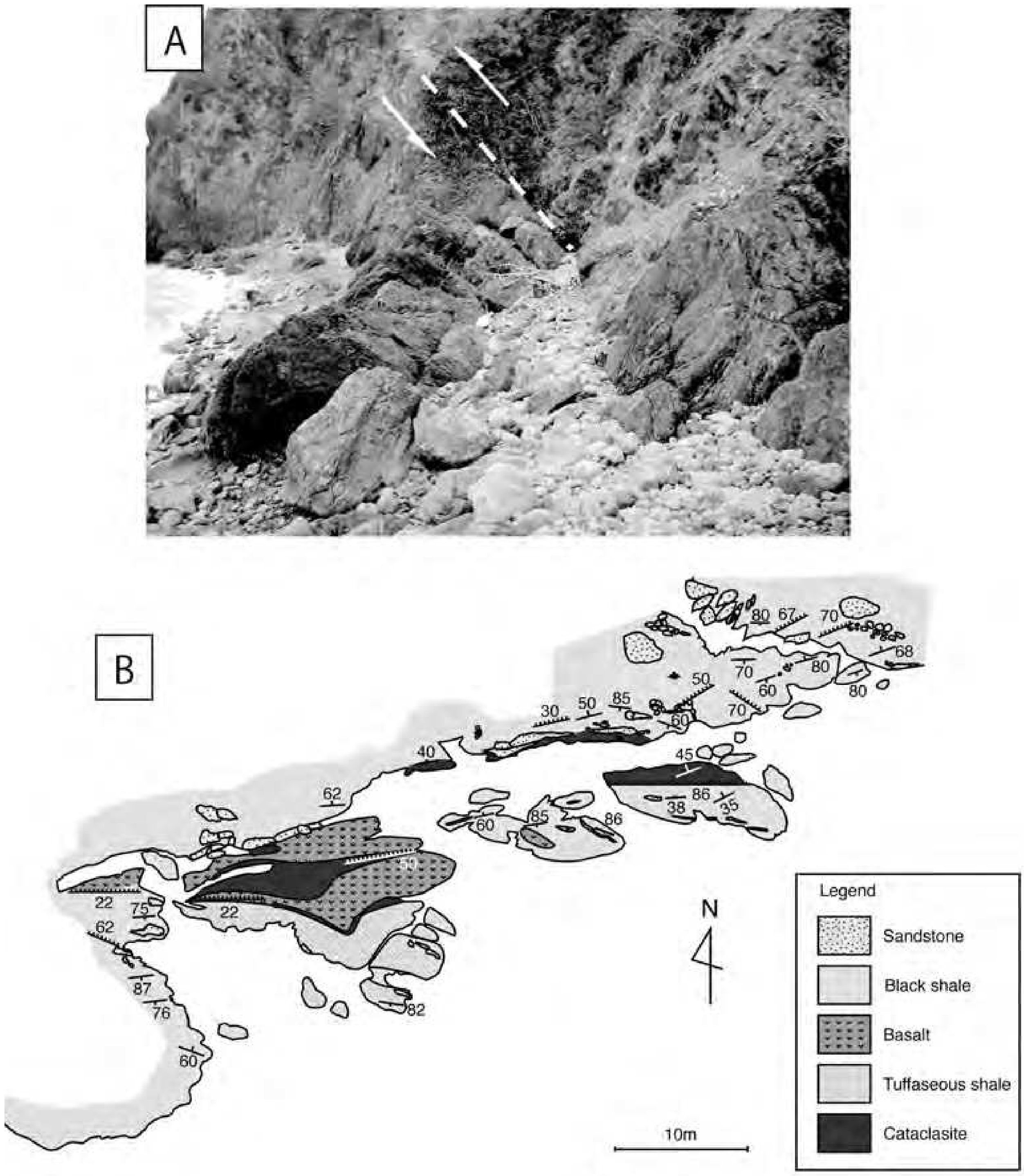

Fig. 2. A) A photo of the study area from ENE to WSW. B) Route map of the northern boundary fault zone between Okitsu melange and Nonokawa formation.

Cataclasites of 2–3 m in thickness are well observed along the fault zone (Fig. 2). The cataclasites include pseudotachylyte, as reported by Ikewasa et al. (2003). They estimated a temperature rise for the fault of at least 450°C, based on the mineral assemblage of the pseudotachylyte.

We focused on two kinds of fault rocks. One is the tectonic melange, as the host rock, and the other is the cataclasites containing pseudotachylyte, as fossil seismogenic fault rocks. The latter type are developped within the host rocks of the tectonic melanges, and thus a comparison of clay minerals in the host rocks and the cataclasites provides the characteristic modification of clay minerals along seismogenic faults.

3. Occurrence of tectonic mélange and Cataclasites with pseudotachylyte

The occurrence of tectonic melanges and cataclasites with pseudotachylyte in outcrop scale is represented in Fig. 3.

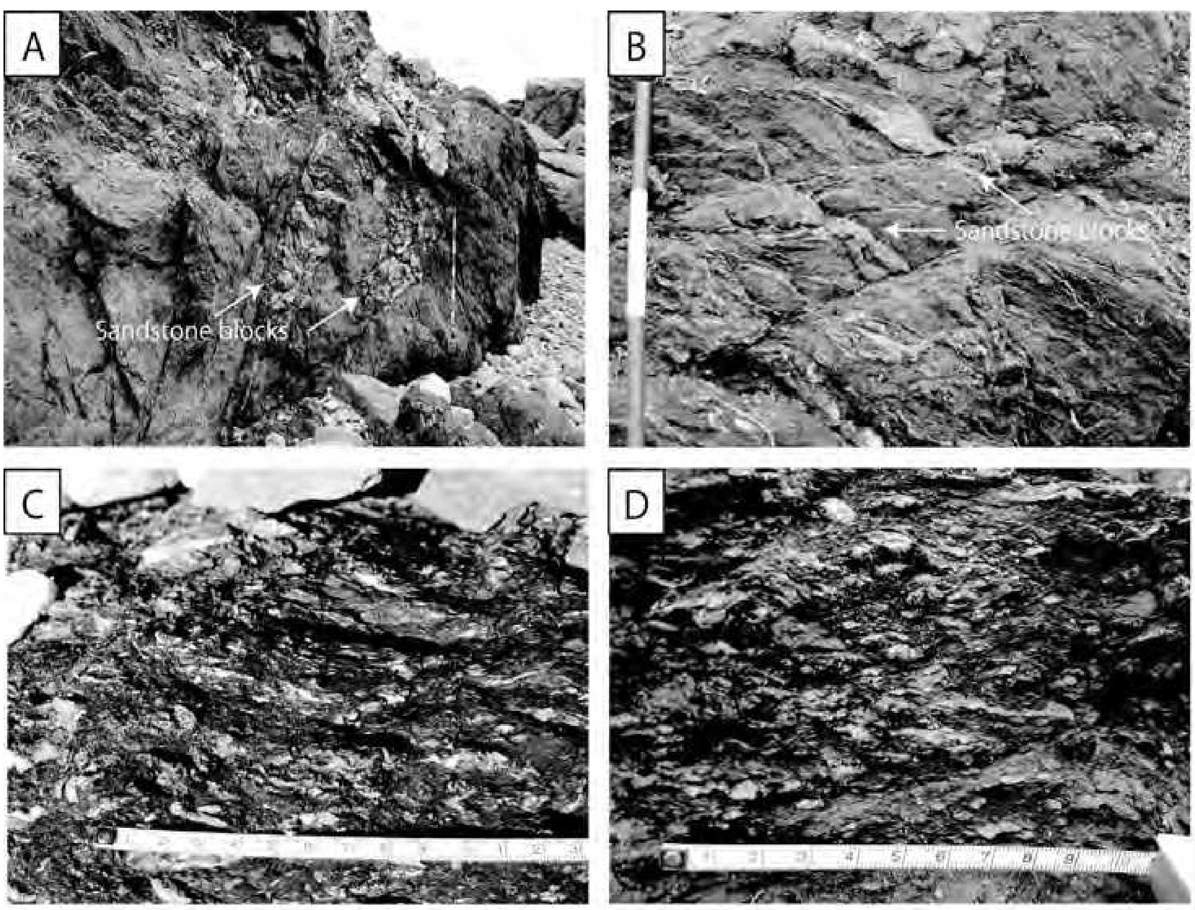

Fig. 3. Occurrences of tectonic melanges (host rocks) and cataclasites with pseudotachylyte in outcrop scale. A) A photo of tectonic melanges. Color bar indicates 1 m length. B) A close-up photo of tectonic melanges. White interval represents 10 cm. C) A photo of cataclasites showing quartz grains surrounded by black matrices. D) A photo of cataclasite. Very thin faults are developed within the cataclasites.

The melanges show blocks in matrix textures, as commonly reported from other tectonic melange zones. The blocks are asymmetrically shaped, indicating that the shear deformation is strongly related to the texture formation (Figs. 3A and B). The melange blocks of sandstone range from a few cm to about 2–3 m in diameter in outcrop scale (Figs. 3A and B).

Foliations are well developed in the shale matrices, representing composite planar fabrics, with the interval between foliations on the scale of mm. Micro-faults, with a thickness of less than 1 cm and a displacement of less than 1 m, can also be observed cutting into the melange fabrics in outcrop scale (Figs. 3A and B). Most of the micro-faults are accompanied by quartz and calcite veins. Some mineral veins in the study area are ankerite (Fe–Mg carbonate). The relationship between the micro-faults and cataclasites containing pseudotachylyte is unknown.

The cataclasites with pseudotachylyte are composed of relatively small grains (less than a few cm diameter) of quartz and calcite surrounded by black material (Figs. 3C and D). These blocks also have an asymmetric shape, and the long axis of the blocks is aligned in the same direction as the melange fabrics (Figs. 3C and D). In some parts, very thin (less than 1 mm), continuous faults are observed within the cataclasites, although these thin faults are obscure (Fig. 3D).

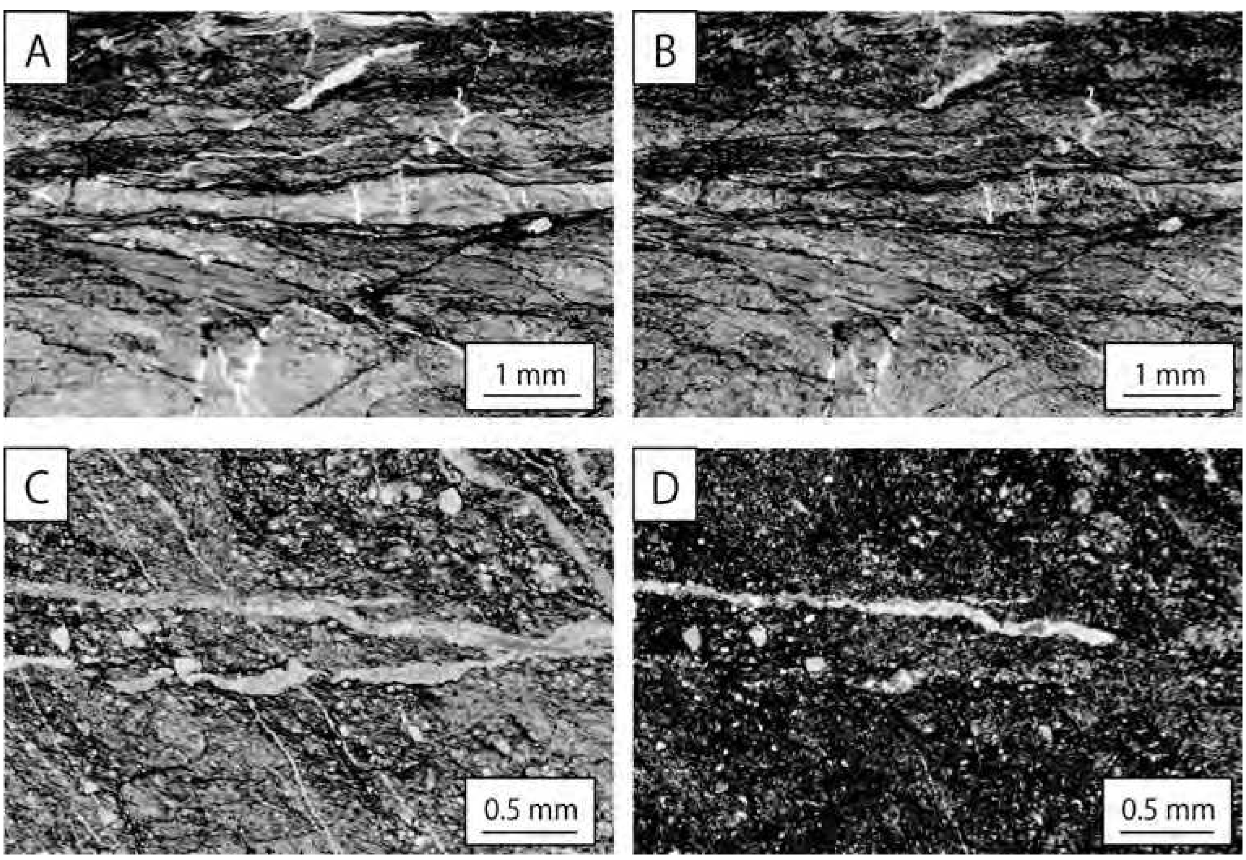

Fig. 4. Micro-textures of tectonic melanges. A) Black seams (Pressure solution cleavages) are well developed in shale matrices. B) A photo of Fig. 4A under cross poralized light. C) Very weak anastomosed pressure solution cleavage in sandy shale matrices. D) A photo of Fig. 4C under cross polarized light.

At the microscopic scale, the occurrence of tectonic melanges and cataclasites with pseudotachylyte is also distinctive.

Microscopic occurrence of tectonic melanges is characterized by a weak pressure solution cleavage within shale matrices (Fig. 4). The pressure solution cleavages develop along melange foliations, also representing composite planar fabrics. In coarser grained areas, pressure solution cleavages are weakly observed, showing anastomosed networks of pressure solution cleavages (Figs. 4C and D).

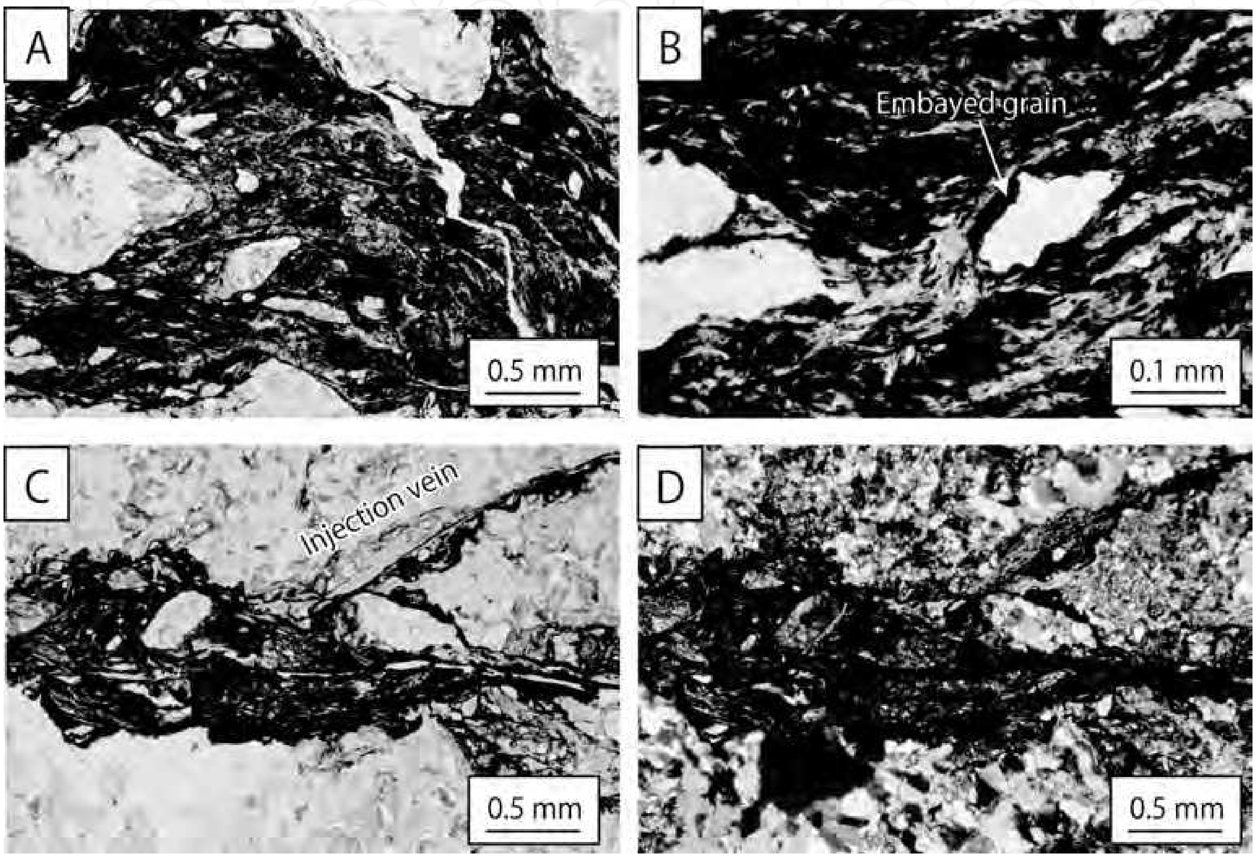

Fig. 5. Micro-texture of cataclasites with pseudotachylyte. A) Quartz grains are surrounded by shale matrices. Thin faults and micro-folding are identified within the shale matrices. B) Embayed grains surrounded by shale matrices. C) Injection vein from main fault surface (Horizontal). The boundary with host rocks is embayed. D) A photo of Fig. 5C under cross-polarized light.

In cataclasites with pseudotachylyte, highly fractured grains surrounded by shale matrices are observed (Figs. 5A and B). The grains are composed mainly of quartz aggregates, with grain size ranging from tens of μm to a few mm. The shale matrices represent highly deformed fabrics with lighter and darker brownish materials (Figs. 5A and B). Very thin and sharp faults are recognized within the shale matrices of the cataclasites (Fig. 5A and B). The shape of grains is embayed (Fig. 5B), and injection veins from the main shear surface can also be seen (Figs. 5C and D). Along the main shear surface, highly fractured cataclasites are observed. The boundary between host rocks and cataclasites shows embayed texture.

Injection veins from the main shear surface also have an embayed boundary with the host rocks (Figs. 5C and D).

4. Method

We analyzed the clay and other minerals using an X-ray diffractometer (MultiFlex, RIGAKU) for randomly oriented and oriented samples. Randomly oriented samples were analyzed for bulk rock samples. The oriented samples were prepared using <1.4 μm grains as clay size fraction. Oriented samples were further analyzed using an ethylenglicoled treatment. The XRD analysis was conducted under the following conditions: 45 kV, 40 mA of Cu kα radiation, step size of 0.01°, and a 2θ range of 2-35°.

From the XRD charts obtained, we examined bulk and clay mineralogy, iron and magnesium substitution in chlorite, and illite crystallinity, and performed a semi-quantification of illite and chlorite in the samples. The peak intensities were obtained using MacDiff 4.2.5. Twenty samples each of tectonic melanges and cataclasites were analyzed.

Illite crystallinity is expressed by a width of the illite 001 peak at half of the peak height above the background for an oriented, < 2 μm fraction of sample (Kubler, 1969). The width is controlled by X-ray-scattering-domain size and percentage of expandable layers (Srodon and Eberl, 1984; Eberl and Velde, 1989). A smaller scattering domain and/or more expandable layers would lead to a wider peak.

The chlorite in the study is Fe–Mg chlorite from both the host melanges and cataclasites with pseudotachylyte, based on the bulk rock analysis. Chlorite is composed of silicate and hydroxide layers, both layers having three sites for positive ions. The substitution of iron and magnesium in the chlorite layers was estimated from the XRD charts, following the method of Moore and Reynolds (1989). I(003)/I(005) gives the symmetry of the Fe distribution (the D value in Moore and Reynolds (1989)) and [I(002) + I(004)]/I(003)′ gives the total number of Fe atoms in six octahedral sites (the Y value in Moore and Reynolds (1989)). I(003)′ is calculated from the following equation (Brown and Brindley, 1980):

$$I(003)' = \frac{I(003)(114)^2}{(114 - 12.1D)^2} \tag{1}$$

Reference frame in the configuration described above for the number of iron and magnesium from 0 to 3 at intervals of 0.5 in the silicate and hydroxide layers (the total number of patterns is 49), respectively, were calculated by NEWMOD (Reynolds Jr, 1985). The results of the NEWMOD calculations in the I(003)/I(005) vs. [I(002) + I(004)]/I(003)′ space are shown in Fig. 7 as dotted lines.

For the semi-quantitative analysis of illite and chlorite, we used the Mineral Intensity Factor (MIF) method (Moore and Reynolds, 1989). To obtain the MIF value, we computed the mineral reference intensities for illite and chlorite also using the NEWMOD (Moore and Reynolds, 1989). As the MIF value for chlorite depends on its composition, we used the result from the examination of iron-magnesium substitution in chlorite described above. We used an illite composition of 0.1 Fe and 0.75 K as a reference mineral. Values of μ* = 14 and sigma* = 25 were used in the NEWMOD calculations, as suggested by Moore and Reynolds (1989).

sample	Chlorite	illite	quartz	calcite	anorthite	ankerite
ok060501-2	X	X	X		X	
ok060501-3	X	X	X	X	X	
ok060902-1	X	X	X	X	X	
ok060902-4	X	X	X		X	
ok060902-5	X	X	X		X	
ok060902-6	X	X	X	X	X	
ok060902-7	X	X	X	X	X	
ok060902-14	X	X	X	X	X	
ok061004-18	X	X	X		X	
ok061004-19	X	X	X	X	X	
ok060501-7	X	X	X	X	X	
ok060616-7	X	X	X	X	X	
ok060620-1	X	X	X	X	X	
ok060902-8	X	X	X	X	X	
ok060919-6	X	X	X		X	
ok060919-7	X	X	X		X	
ok060919-8	X	X	X		X	
ok060919-9	X	X	X		X	
ok060919-10	X	X	X		X	
ok060919-11	X	X	X		X	

Table 1. Minerals in host melanges

sample	Chlorite	illite	quartz	calcite	anorthite	ankerite
ok060428-2	X	X	X		X	
ok060620-4	X	X	X		X	
ok060620-13	X	X	X		X	
ok060902-13	X	X	X		X	
ok061015-7	X	X	X		X	
ok061015-8	X	X	X		X	
ok061015-9	X	X	X		X	
ok061015-10	X	X	X	X	X	
ok061015-11	X	X	X	X	X	
ok061015-12	X	X	X	X	X	
ok060501-8	X	X	X	X	X	
ok060616-4	X	X	X	X	X	
ok060902-9	X	X	X	X	X	
ok060902-12	X	X	X	X	X	
ok060919-12	X	X	X	X	X	
ok061004-23	X	X	X	X	X	
ok061004-24	X	X	X	X	X	
ok061004-25	X	X	X	X	X	X
ok061004-26	X	X	X		X	
ok061004-27	X	X	X	X	X	X

Table 2. Minerals in cataclasites with pseudotachylyte

5. Results

In this section, we describe the results of our analysis for clay and other mineralogy, iron and magnesium substitution in chlorite, illite crystallinity, and the semi-quantification of illite and chlorite.

5.1 Clay and other mineralogy

All samples, from both the host melanges and the cataclasites, included quartz, anorthite, illite, and chlorite (Tables 1 and 2), and some of the samples also contained calcite. Ankerite (Fe–Mg carbonates) were found in a number of samples from cataclasites with pseudotachylyte (Tables 1 and 2). On the basis of the bulk powder analysis for XRD, the chlorite are Fe–Mg chlorite. The results from samples analyzed by ethylenglicoled treatment suggest that smectite is not present in any sample (Fig. 6).

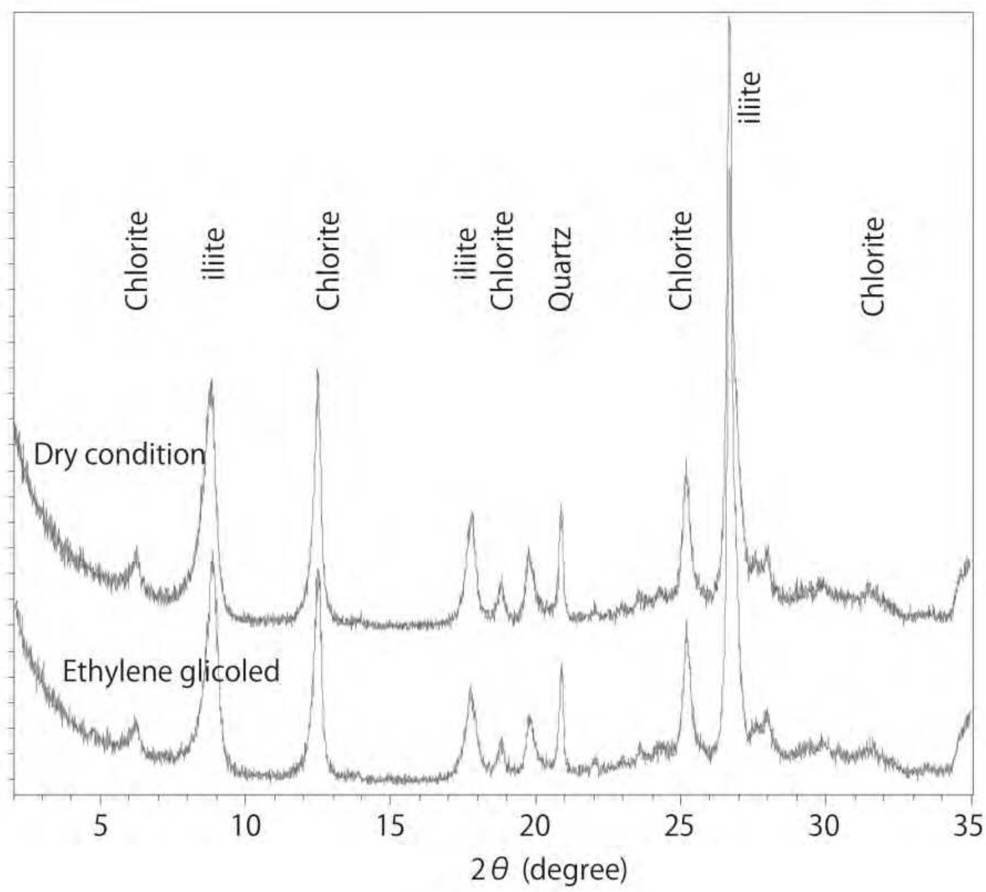

Fig. 6. Examples of XRD charts for oriented samples of cataclasites with pseudotachylyte.

5.2 Iron and magnesium substitution in chlorite

Iron and magnesium substitution in chlorite is shown in Fig. 7. The x-axis indicates I(003)/I(005), related to the D value, and the y-axis indicates [I(002) + I(004)]/I(003)′, related to the Y value. In this parameter space, the amount of iron in the hydroxide and silicate layers is shown by dotted lines. For host tectonic melanges, the iron content in both hydroxide and silicate layers is relatively higher than that in the cataclasite samples. The iron content in the host tectonic melanges is distributed over a wide area (Fig. 7). In contrast, these plots show that the iron in cataclasites with pseudotachylyte is concentrated in a smaller area around smaller iron content of both the hydroxide and silicate layers.

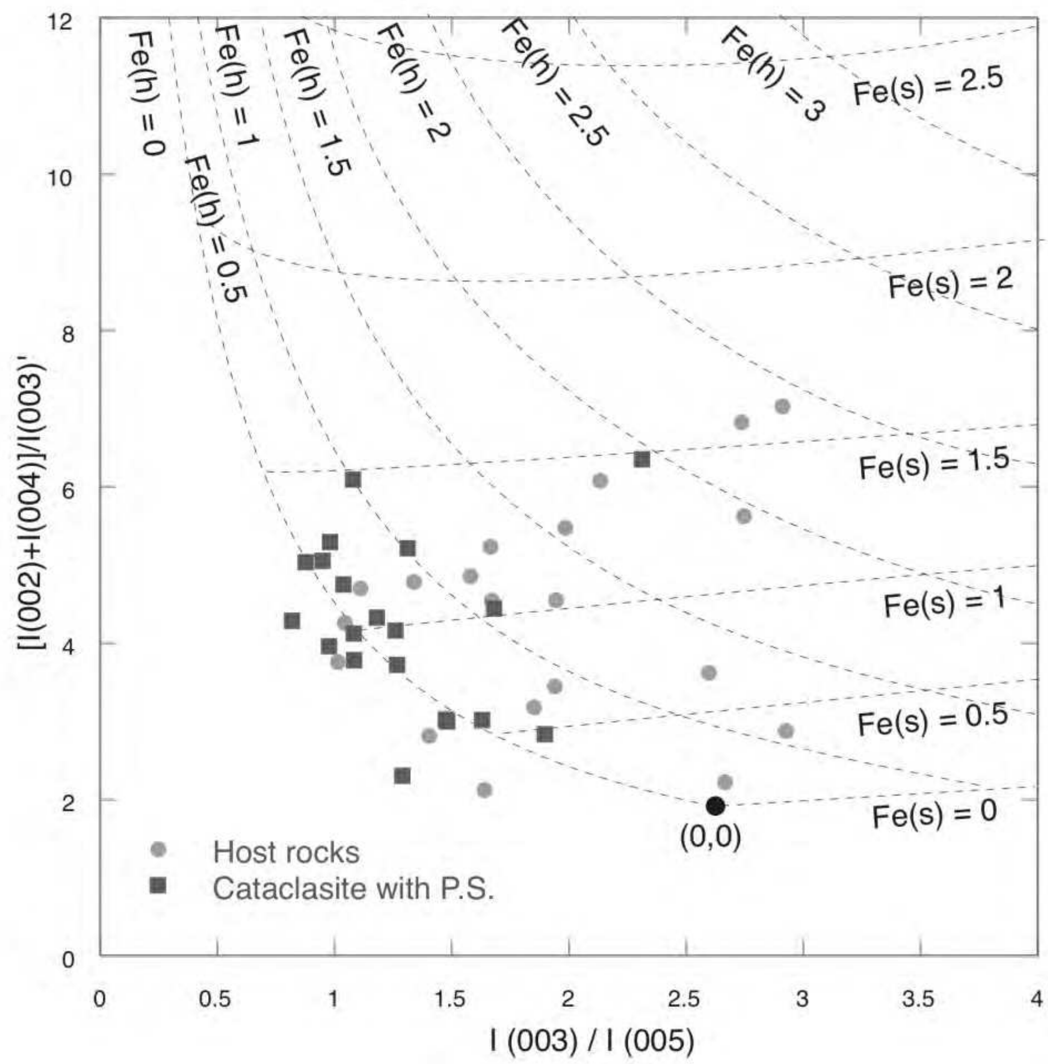

Fig. 7. A diagram of the Fe–Mg substitution of chlorite.

5.3 Illite crystallinity

The illite crystallinity of the tectonic mélange and cataclasites samples is shown in Fig. 8. The host melange samples have an illite crystallinity ranging from about 0.3 to 0.46, with an average value of about 0.4. Illite crystallinity in the cataclasites with pseudotachylyte varies from 0.41 to 0.58, averaging around 0.46. The larger values of crystallinity suggest that the illite in cataclasites is less crystallized than in the host melanges.

5.4 Semi-quantification between illite and chlorite

The semi-quantification of illite and chlorite was conducted using the MIF method, as described above. The results are shown in Fig. 8. The illite ratio to chlorite for host rocks ranges from about 20 wt% to about 70 wt%, with an average value of 46 wt%. The same ratio in cataclasites with pseudotachylyte varies from 40 wt% to 90 wt%, with an average of 65 wt% (Fig. 8). The illite to chlorite ratio is larger in cataclasites than the host melanges, suggesting that the amount of illite increases in cataclasites if the amount of chlorite is constant, or the amount of chlorite decreases relative to the amount of illite.

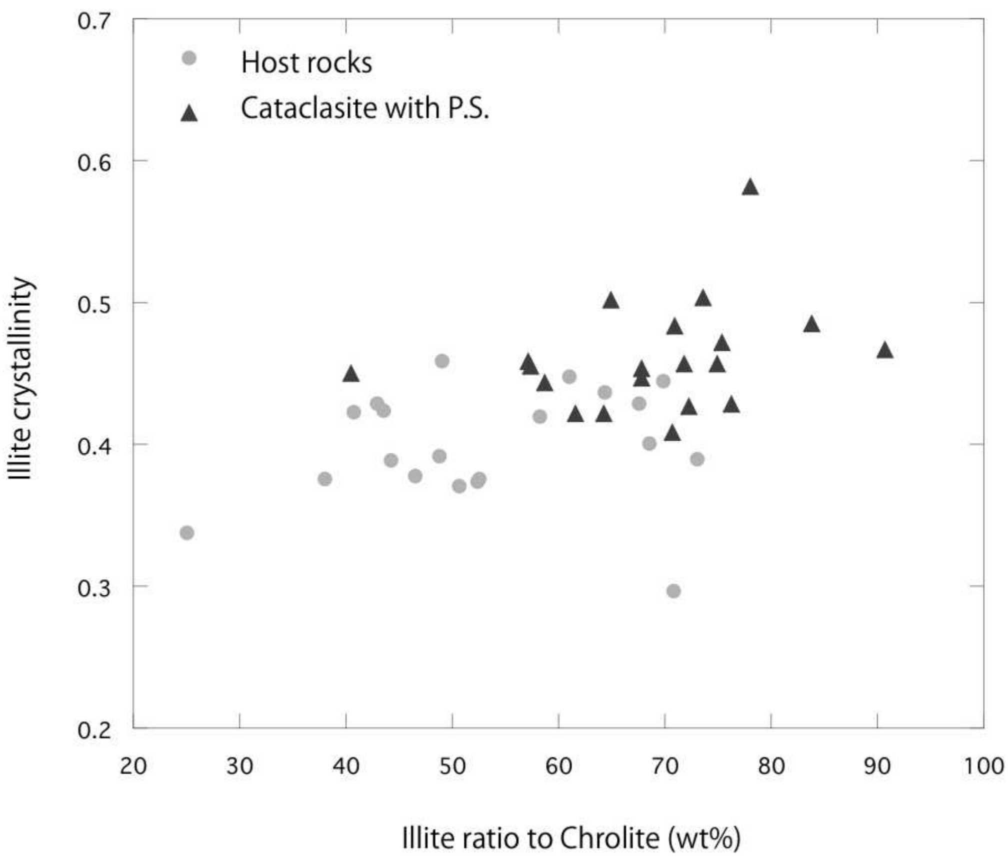

Fig. 8. Illite ratio to chlorite (wt%) vs. illite crystallinity for host rocks and cataclasites with pseudotachylyte

6. Discussions

6.1 Iron consumption in chlorite in cataclasites with pseudotachylyte

In chlorite from cataclasites with pseudotachylyte, the iron content is decreased in both the hydroxide and silicate layers, compared with host melanges, as described above (Fig. 7). The same trend has been reported in the Taiwan Chelung-pu fault (Hashimoto et al., 2007; Hashimoto et al., 2008); however, the initial state of the host rocks in Taiwan is different from those studied here. Although host rock samples from Chelung-pu fault displayed greater iron content than the Okitsu samples, fault rocks from both areas showed a decreased level of iron in their chlorite.

The decrease of iron in chlorite from fault rocks can be controlled by the temperature of the source fluid (Ohta and Yajima, 1988), the pH of the fluid (Malmstrom et al., 1996; Ross, 1969), or lithology (host rocks), as discussed in Hashimoto et al. (2008). Because the same trend of a decrease of iron levels in fault rocks was observed from different host rocks, lithology control is less significant. Ohta and Yajima (1988) reported that higher temperature is related to higher iron content in chlorite in hydrothermal environments, which is the opposite trend to that observed in our analysis, as fault rocks are expected to experience higher temperatures due to frictional heating. Therefore, temperature rise cannot explain the decrease in iron from chlorite in fault rocks. The pH of the source fluid is thus the most likely cause of the decreased iron content in chlorite from fault rocks. The change in pH of the fluid can be caused by radical reactions; that is, the reactions between water and newly created surfaces of minerals due to the breakage of mineral grains. Laboratory experiments on radical reactions showed that the pH of a fluid could be decreased or increased by the breakage of quartz, feldspar, and micas (Kameda et al., 2003; Saruwatari et al., 2004). The change in pH of fluid depends on a complex series of interactions with the broken minerals, and is thus difficult to understand quantitatively outside the laboratory.

The decrease of iron content in ultracataclasites with pseudotachylyte has also been observed in isocon diagrams from a bulk chemical analysis at another fault zone (the Mugi melange, Cretaceous Shimanto Belt, Shikoku, SW Japan; see Hashimoto et al., 2009). This suggests that the characteristic pH of the source fluid can be related to iron consumption from host rocks. The consumed iron from host rocks is observed within minerals precipitated from related fluid. Ankerite veins (Fe–Mg carbonates) are concentrated in seismogenic faults, such as the Okitsu fault described in this study.

6.2 Higher illite crystallinity and illite content in cataclasites with pseudotachylyte

The illite crystallinity of cataclasites with pseudotachylyte had a higher value than that of host melanges. Illite crystallinity is commonly used as an index of paleo-maximum Temperature (e.g., Guithrie et al., 1986; Awan and Kimura, 1996), with higher illite crystallinity indicating a lower paleo-maximum temperature. The cataclasites with pseudotachylyte are expected to have been subjected to a higher paleo-maximum temperature than the host rocks, due to frictional heating. Ikesawa et al. (2003) estimated the minimum temperature from frictional heating to be about 450°C on the basis of the composition of pseudotachylytes. Therefore, the higher illite crystallinity in cataclasites cannot be interpreted by the paleo-maximum temperature. Theoretically, illite crystallinity is controlled by X-ray-scattering–domain size and percentage of expandable layers (Srodon and Eberl, 1984; Eberl and Velde, 1989). As the illite in this study did not include expandable layers within it, the effect of the percentage of expandable layers on the crystallinity is negligible. A wider peak (higher illite crystallinity) indicates a smaller scattering domain. Therefore, the higher value of illite crystallinity for cataclasites with pseudotachylyte indicates that the particle size of illite is smaller than that of host melanges. Possible mechanisms for making smaller illite particles include comminution during cataclastic deformation, and a smaller size of authigenic illite formation related to pseudotachylyte formation.

The semi-quantitative analysis to examine the ratio of illite and chlorite indicates that the proportion of illite increases in cataclasites with pseudotachylyte, compared with that in host mélanges. This result suggests either an increase of illite or a decrease of chlorite in cataclasites. The chemical analysis and mineralogical observations of pseudotachylyte in sedimentary rocks indicates that the melt mainly originates from clay minerals, and quartz and feldspar grains that are resistant to melting (Ujiie et al., 2007). This resistance is due to differences in melting temperatures between clay and other minerals in sedimentary rocks. As it might be difficult to melt chlorite selectively, the increase in the illite ratio might be related to the authigenic illite through pseudotachylyte formation.

Smectite concentrations have been reported from the seismogenic fault zone in the Chelung-pu fault, Taiwan (Kuo et al., 2009). It was found that the smectite in the fault zone does not include an illite-smectite mixed layer, and this was interpreted as meaning that the smectite can be formed by alteration of glass (pseudotachylyte) (Kuo et al., 2009). The Chi-Chi earthquake occurred in 1999, and the Taiwan Chelung-pu fault Drilling Project (TCDP) was conducted in 2004. Within that 5-year interval, the alteration of glass to form smectite could have been progressed. Such alteration to form smectite from glass matrices in pseudotachylyte is also expected in the Okitsu examples. The formation of smectite might also be a significant rock-fluid interaction along a seismogenic fault.

The authigenic smectite is transformed to illite due to diagenetic processes. Smectite-illite transition proceeds with temperature, and the illitization is almost complete at 150°C (Moore and Vrolijk, 1992). Therefore, the smectite from pseudotachylyte glass could be transformed to illite. The illitization from authigenic smectite can also be related to a smaller size of illite, as identified by the larger value of illite crystallinity in cataclasites with pseudotachylyte. The linear relationship between the illite to chlorite ratio and illite crystallinity can be seen in Fig. 8, indicating that a larger illite ratio is associated with a smaller illite grain size. The relationship might also be explained by the illitization of authigenic smectite.

During illitization, the interlayer of smectite is dewatered. The water should migrate to the fault zone after a few years of seismogenesis.

Frictional behaviors of smectites and illites have been reported from laboratory experiments in a sliding velocity range from 0.1 to 200 μm (Saffer and Marone, 2003). While smectite indicates velocity weakening at low normal stress, illite represents only velocity strengthening behavior in the wide range of experiments. The velocity strengthening behavior in illite is not supported by the hypothesis that the smectite-illite transition is related to seismogenesis at the seismic front, as suggested by Hyndman et al (1999). Rather, illitization makes faults aseismic (Saffer and Marone, 2003). The illite concentration in cataclasites with pseudotachylyte in this study suggests that the rock-fluid interactions along a seismogenic fault, such as smectite formation from the glass of pseudotachylyte, and illitization from the authigenic smectite, are processes that modify the fault to an aseismic fault.

7. Conclusion

The iron content in chlorite in cataclasites with pseudotachylyte is smaller than that of tectonic melanges (host rocks), as observed in other seismogenic fault rocks. The decrease of iron in chlorite suggests that a specific pH fluid reacted with fault rocks due to radical reactions.

Illite crystallinity in cataclasites is higher than in host rocks. In addition, the relative amount of illite is increased in cataclasites compared with host rocks. These results imply that the smectite altered from glass in pseudotachylyte transformed into illite along a seismogenic fault.

8. Acknowledgment

We thank Prof. Higashi, M. for the help in XRD analysis. We also appreciate Dr. Kameda, J. for his constructive discussions.

9. References

Awan, M. A. & Kimura, K. (1996). *Thermal structure and uplift of the Cretaceous Shimanto Belt, Kii Peninsula, Southwest Japan: An illite crystallinity and Illiteq bo, lattice spacing study*, Island Arc, v. 5, no. 1, p. 69-88.

Brodsky, E. E. & Kanamori, H. (2001). *Elastohydrodynamic lubrication of faults*, Journal of Geophysics Research, v. 106, no. 16, p. 357-16.

Brown, G. & Brindley, G. W. (1980). X-ray diffraction procedures for clay mineral identification, Crystal structures of clay minerals and their X-ray identification, v. 5, p. 305-359.

Di Toro, G., Hirose, T., Nielsen, S., Pennacchioni, G. & Shimamoto, T. (2006). *Natural and experimental evidence of melt lubrication of faults during earthquakes*, Science, v. 311, no. 5761, p. 647-649.

Eberl, D. D. & Velde, B. (1989). *Beyond the Kubler index*, Clay Minerals, v. 24, no. 4, p. 571-577.

Guthrie, J. M., Houseknecht, D. W. & Johns, W. D. (1986). *Relationships among vitrinite reflectance, illite crystallinity, and organic geochemistry in Carboniferous strata, Ouachita Mountains, Oklahoma and Arkansas*, AAPG Bulletin, v. 70, no. 1, doi: 10.1306/9488561A-1704-11D7-8645000102C1865D.

Hashimoto, Y. & Kimura, G. (1999). *Underplating process from melange formation to duplexing: Example from the Cretaceous Shimanto Belt, Kii Peninsula, southwest Japan*, Tectonics, v. 18, no. 1, p. 92-107.

Hashimoto, Y., Ujiie, K., Sakaguchi, A. & Tanaka, H. (2007). *Characteristics and implication of clay minerals in the northern and southern parts of the Chelung-pu fault, Taiwan, Tectonophysics*, v. 443, no. 3-4, p. 233-242.

Hashimoto, Y., Tadai, O., Tanimizu, M., Tanikawa, W., Hirono, T., Lin, W., Mishima, T., Sakaguchi, M., Soh, W. & Song, S. R. (2008). *Characteristics of chlorites in seismogenic fault zones: the Taiwan Chelungpu Fault Drilling Project (TCDP) core sample*, eEarth, v. 3, no. 1, p. 1-6.

Hashimoto, Y., Nikaizo, A. & Kimura, G. (2009). *A geochemical estimation of fluid flux and permeability for a fault zone in Mugi melange, the Cretaceous Shimanto Belt, SW Japan*, Journal of Structural Geology, v. 31, no. 2, p. 208-214.

Honda, G., Ishikawa, T., Hirono, T. & Mukoyoshi, H. (2011). *Geochemical signals for determining the slip-weakening mechanism of an ancient megasplay fault in the Shimanto accretionary complex*, Geophysical research letters, v. 38, no. 6, doi:10.1029/2011GL046722.

Hyndman, R. D. & Wang, K. (1993). *Thermal constraints on the zone of major thrust earthquake failure: The Cascadia subduction zone*, Journal of Geophysical Research, v. 98, no. B2, p. 2039-2060.

Ikesawa, E., Sakaguchi, A. & Kimura, G. (2003). *Pseudotachylyte from an ancient accretionary complex: Evidence for melt generation during seismic slip along a master d collement?*, Geology, v. 31, no. 7, p. 637-640.

Ishikawa, T., Tanimizu, M., Nagaishi, K., Matsuoka, J., Tadai, O., Sakaguchi, M., Hirono, T., Mishima, T., Tanikawa, W. & Lin, W. (2008). *Coseismic fluid-rock interactions at high temperatures in the Chelungpu fault*, Nature Geoscience, v. 1, no. 10, p. 679-683.

Kameda, J., Saruwatari, K. & Tanaka, H. (2003). *H2 generation in wet grinding of granite and single-crystal powders and implications for H2 concentration on active faults*, Geophysical research letters, v. 30, no. 20, doi:10.1029/2003GL018252.

Kano, Y., Mori, J., Fujio, R., Ito, H., Yanagidani, T., Nakao, S. & Ma, K. F. (2006). *Heat signature on the Chelungpu fault associated with the 1999 Chi-Chi, Taiwan earthquake*, Geophys. Res. Lett, v. 33, L14306, doi:10.1029/2006GL026733.

Kimura, G. & Mukai, A. (1991). *Underplated units in an accretionary complex: Melange of the Shimanto Belt of eastern Shikoku, southwest Japan*, Tectonics, v. 10, no. 1, p. 31-50.

Kubler, B. (1969). *Crystallinity of illite, Detection of metamorphism in some frontal parts of the Alps:* Fortschr. der Mineralogie, v. 47, p. 39-40.

Kuo, L. W., Song, S. R., Yeh, E. C. & Chen, H. F. (2009). *Clay mineral anomalies in the fault zone of the Chelungpu Fault, Taiwan, and their implications*, Geophysical research letters, v. 36, no. 18, doi:10.1029/2009GL039269.

Malmstrom, M., Banwart, S., Lewenhagen, J., Duro, L. & Bruno, J. (1996). *The dissolution of biotite and chlorite at 25˚C in the near-neutral pH region*, Journal of contaminant hydrology, v. 21, no. 1-4, p. 201-213.

Mase, C. W. & Smith, L. (1987). *Effects of frictional heating on the thermal, hydrologic, and mechanical response of a fault*, Journal of Geophysical Research, v. 92, no. B7, p. 6249-6272.

Melosh, H. J. (1979). *Acoustic fluidization-A new geologic process*, Journal of Geophysical Research, v. 84, p. 7513-7520.

Mishima, T., Hirono, T., Soh, W. & Song, S. R. (2006). *Thermal history estimation of the Taiwan Chelungpu fault using rock-magnetic methods*, Geophysical research letters, v. 33, no. 23, doi:10.1029/2006GL028088.

Moore, D. M. & Reynolds, R. C. (1989). X-ray Diffraction and the Identification and Analysis of Clay Minerals. Oxford University Press, Wellington, pp. 348.

Moore, J. C. & Vrolijk, P. (1992). *Fluids in accretionary prisms*, Reviews of Geophysics, v. 30, no. 2, p. 113-135.

O'Hara, K., Mizoguchi, K., Shimamoto, T. & Hower, J. C. (2006). *Experimental frictional heating of coal gouge at seismic slip rates: Evidence for devolatilization and thermal pressurization of gouge fluids*, Tectonophysics, v. 424, no. 1-2, p. 109-118.

Ohta, E. & Yajima, J. (1988). *Magnesium to Iron Ratio of Chlorite as Indicator of Type of Hydrothermal Ore Deposits*, Mining Geology, Special Issue, v. 12, p. 17–22.

Oleskevich, D. A., Hyndman, R. D. & Wang, K. (1999). *The updip and downdip limits to great subduction earthquakes: Thermal and structural models of Cascadia, south Alaska, SW Japan, and Chile*, Journal of Geophysical Research, v. 104, no. B7, p. 14965-14991.

Onishi, C. T. & Kimura, G. (1995). *Melange fabric and relative convergence in subduction zone*, Tectonics, v. 14, p. 1273-1289.

Otsuki, K., Monzawa, N. & Nagase, T. (2003). *Fluidization and melting of fault gouge during seismic slip: Identification in the Nojima fault zone and implications for focal earthquake mechanisms*, J. Geophys. Res, v. 108, doi:10.1029/2001JB001711.

Reynolds Jr, R. C. (1985). NEWMOD, a computer program for the calculation of one-dimensional diffraction patterns of mixed-layered clays, R. C. Reynolds, Jr., 8 Brook, Dr., Hanover, New Hampshire, 03755.

Ross, G. J. (1969). *Acid dissolution of chlorites: release of magnesium, iron and aluminum and mode of acid attack*, Clays and Clay Minerals, v. 17, p. 347-354.

Saffer, D. M. & Marone, C. (2003). *Comparison of smectite-and illite-rich gouge frictional properties: application to the updip limit of the seismogenic zone along subduction megathrusts*, Earth and Planetary Science Letters, v. 215, no. 1-2, p. 219-235.

Saruwatari, K., Kameda, J. & Tanaka, H. (2004). *Generation of hydrogen ions and hydrogen gas in quartz-water crushing experiments: an example of chemical processes in active faults*, Physics and chemistry of minerals, v. 31, no. 3, p. 176-182.

Sibson, R. H. (1975). *Generation of pseudotachylyte by ancient seismic faulting*, Geophysical Journal of the Royal Astronomical Society, v. 43, no. 3, p. 775-794.

Sibson, R. H. (1977). *Fault rocks and fault mechanisms*, Journal of the Geological Society, v. 133, no. 3, p. 191-213.

Spray, J. G. (1992). *A physical basis for the frictional melting of some rock-forming minerals*, Tectonophysics, v. 204, no. 3-4, p. 205-221.

Srodon, J. & Eberl, D. D. (1984). *Illite*, Reviews in Mineralogy and Geochemistry, v. 13, no. 1, p. 495-544.

Taira, A., Katto, J., Tashiro, M., Okamura, M. & Kodama, K. (1988). *The Shimanto belt in Shikoku, Japan evolution of Cretaceous to Miocene accretionary prism*, Modern Geology, v. 12, no. 5, p. 5-46.

Tanaka, H., Chen, W. M., Wang, C. Y., Ma, K. F., Urata, N., Mori, J. & Ando, M. (2006). *Frictional heat from faulting of the 1999 Chi-Chi, Taiwan earthquake*, Geophysical research letters, v. 33, no. 16, L16316, doi:10.1029/2006GL026673.

Tanaka, H., Omura, K., Matsuda, T., Ikeda, R., Kobayashi, K., Murakami, M. & Shimada, K. (2007). *Architectural evolution of the Nojima fault and identification of the activated slip layer by Kobe earthquake*, Journal of Geophysical Research, v. 112, no. B7, B07304, doi:10.1029/2005JB003977.

Ujiie, K., Yamaguchi, H., Sakaguchi, A. & Toh, S. (2007). *Pseudotachylytes in an ancient accretionary complex and implications for melt lubrication during subduction zone earthquakes*, Journal of Structural Geology, v. 29, no. 4, p. 599-613.

Wibberley, C. A. J. & Shimamoto, T. (2005). *Earthquake slip weakening and asperities explained by thermal pressurization*, Nature, v. 7051, p. 689-692.

Yamaguchi, A., Cox, S. F., Kimura, G. & Okamoto, S. (2011). *Dynamic changes in fluid redox state associated with episodic fault rupture along a megasplay fault in a subduction zone*, Earth and Planetary Science Letters, v. 302, no. 3-4, p. 369-377.

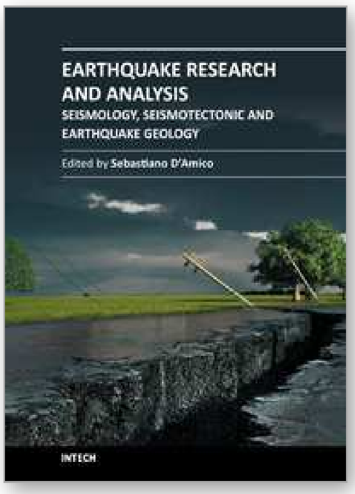

Earthquake Research and Analysis - Seismology, Seismotectonic and Earthquake Geology
Edited by Dr Sebastiano D'Amico

ISBN 978-953-307-991-2
Hard cover, 370 pages
Publisher InTech
Published online 08, February, 2012
Published in print edition February, 2012

This book is devoted to different aspects of earthquake research. Depending on their magnitude and the placement of the hypocenter, earthquakes have the potential to be very destructive. Given that they can cause significant losses and deaths, it is really important to understand the process and the physics of this phenomenon. This book does not focus on a unique problem in earthquake processes, but spans studies on historical earthquakes and seismology in different tectonic environments, to more applied studies on earthquake geology.